

ChemComm

Accepted Manuscript



This is an *Accepted Manuscript*, which has been through the Royal Society of Chemistry peer review process and has been accepted for publication.

Accepted Manuscripts are published online shortly after acceptance, before technical editing, formatting and proof reading. Using this free service, authors can make their results available to the community, in citable form, before we publish the edited article. We will replace this *Accepted Manuscript* with the edited and formatted *Advance Article* as soon as it is available.

You can find more information about *Accepted Manuscripts* in the [Information for Authors](#).

Please note that technical editing may introduce minor changes to the text and/or graphics, which may alter content. The journal's standard [Terms & Conditions](#) and the [Ethical guidelines](#) still apply. In no event shall the Royal Society of Chemistry be held responsible for any errors or omissions in this *Accepted Manuscript* or any consequences arising from the use of any information it contains.

Studying Localized Corrosion using Liquid Cell Transmission Electron Microscopy

Cite this: DOI: 10.1039/x0xx00000x

See Wee Chee^a, Sarah H. Pratt^b, Khalid Hattar^b, David Duquette^a, Frances M. Ross^c, and Robert Hull^a

Received 00th January 2012,
Accepted 00th January 2012

DOI: 10.1039/x0xx00000x

www.rsc.org/

Localized corrosion of Cu and Al thin films exposed to aqueous NaCl solutions was studied using liquid cell transmission electron microscopy (LCTEM). We demonstrate that potentiostatic control can be used to initiate pitting and that local compositional changes, due to focused ion beam implantation of Au⁺ ions, can modify the corrosion susceptibility of Al films.

A liquid platform for performing electrochemical experiments *in situ* within the transmission electron microscope (TEM) was first demonstrated by Williamson *et al.*¹ and was used for direct observations of the electrodeposition of Cu from solution. A key feature was the use of standard semiconductor microfabrication techniques to construct the microfluidic cell. Since then, liquid cell electron microscopy has seen rapid development and application, particularly in the areas of electrochemistry^{2–6} and nanoparticle dynamics⁷. Liquid cell TEM (LCTEM) work by sandwiching a fluid layer between electron-transparent and impermeable membranes (e.g. silicon nitride) fabricated on chips, which are separated by a spacer typically a few hundred nanometers in height. Hermetic sealing of the liquid cell isolates fluids from the vacuum of the TEM column. Liquid dynamics within the cell may be manipulated by an external pump if flow channels are integrated into the TEM holder. Electrical connections can be made to the sample via wiring that pass through the holder and make contact with thin film electrodes patterned within the cell. Recent reports demonstrated real-time electrochemical studies of the solid-electrolyte interphases⁶ in lithium ion battery electrodes and of lithiation processes^{3–5}.

The corrosion of metals and alloys is another branch of electrochemistry where LCTEM can have significant impact. Developing a complete understanding of localized corrosion remains one of the fundamental challenges in corrosion science. Metals exhibiting passivity, such as aluminum alloys and stainless steels, commonly suffer from localized corrosion, especially pitting corrosion. Pitting is caused by local breakdown of the protective oxide film leading to accelerated dissolution of the underlying metal⁸. However, with existing experimental techniques, it can be challenging to probe the early stages of pitting⁹. Difficulties include the small dimensions of pit initiation events, the rare and stochastic nature of these events, the rapid and dynamic nature of pit growth

immediately after initiation, and the chemical characterization of the surface film within aqueous environments at length scales comparable with the pit dimensions. LCTEM, coupled with potentiostatic control, has tantalizing potential to provide insight into pit initiation events. One can resolve nanometer size features in LCTEM, even when achievable resolution is degraded by imaging through the liquid layer^{10,11}. Elemental characterization of corrosion products is also possible. Recent studies have demonstrated the feasibility of chemical analysis using energy dispersive x-ray spectroscopy^{12,13} (EDX) and electron energy loss spectroscopy^{2,14} (EELS) in liquid samples.

In this paper, we show images obtained during pitting corrosion of metal films induced by aqueous sodium chloride (NaCl) solutions. Two materials were chosen, Cu because of its relatively high resistance to corrosion, leading to widespread use in water systems, and Al, because it is a model system for pitting corrosion that includes an extensive literature of *ex situ* observations, which can be compared with *in situ* results. We show that LCTEM experiments produce corrosion damage similar to those seen *ex situ*, and identify different morphologies in Al. We then present results aimed at controlling the onset of pitting. We first show the initiation of corrosion by applying a potential to an Al film. Second, we show that compositional changes can be used to modify corrosion susceptibility. Compositional modulations were introduced by patterning an Al film with a focused ion beam of Au ions. Finally, based on these results, we discuss the experimental considerations in performing corrosion studies using LCTEM in the supplementary information (ESI†). For example, the sample must meet the thickness requirement for TEM imaging, in addition to fulfilling the design considerations of a standard electrochemical experiment. The microfluidic cell imposes limitations in terms of sample geometry and electrochemical cell design. Use of corrosive fluids can damage the holder and even the microscope. In spite of the experimental challenges, we conclude that LCTEM can provide detailed and unique information during the onset of corrosion processes.

Figure 1 illustrates corrosion morphologies observed in Cu and Al films after exposure to aqueous NaCl solutions. Experimental details are presented in the ESI†. Images from a 50 nm thick Cu film under flow of a 6M NaCl solution are presented in the first row (a-c). After two hours of liquid flow, pits with sizes of a few hundred

nanometers and in different stages of development are visible in the copper film. The growth of an existing pit can also be tracked in real time. A representative movie is provided in Movie S1 (ESI†). The images and movies suggest that corrosion occurs via the dissolution of individual grains for Cu. While it is known that Cu will pit under certain conditions, the mechanism of pitting remains poorly understood¹⁵. The susceptibility of Cu to pitting can be influenced by HCO_3^- , SO_4^{2-} , and Cl^- ions¹⁶. For Cl^- ions, pitting behavior shows a complex dependence on the concentration because it controls both oxide film formation and pit initiation via the formation of CuCl ¹⁷.

In the experiments shown here, the dissolution rate appear to accelerate when a condensed beam and high electron dose is used. It is clearly important to quantify the role of radiolysis by the electron beam on any corrosion reaction under investigation. Radiolysis of aqueous NaCl solutions by energetic particles is known to create species such as HClO^\cdot ¹⁸, which can turn the solutions oxidizing via formation of hypochlorite¹⁹. Hence, the dose rates used in TEM can strongly alter the solution chemistry^{20–22}. Simulations (see ESI†) show that under standard imaging conditions used in the current experiments, the concentration of HClO^\cdot remains low. If the dose rate is increased, it may be necessary to consider the effects of HClO^\cdot and other radiolysis products when interpreting data.

In contrast, Al is known to only pit in the presence of halide ions such as Cl^- . This process can be tracked in the liquid cell, and has been reported in Refs. ²³ and ²⁴. Figure 1 (d-l) shows representative results. Two prototypical structures found in Al thin film corrosion are reproduced in the *in situ* TEM experiments. Blisters (d-f), observed after exposure to 0.01 M NaCl solutions, and meandering corrosion tracks (g-i) observed in 1 M solutions. Single pits were also found in the film exposed to 1 M NaCl solution (j and k). Post-mortem images taken with a light microscope (l) show that (i) was an extension of a propagating fractal-like corrosion pattern, whereas (k) belonged to a region of intact film that had begun to pit. Also, note the relatively long times (at least a few hours) required to induce visible corrosion, with the time needed increasing for lower NaCl concentrations. To limit electron dose to the sample during these time periods, development of the film microstructure was observed in snapshots, i.e. at intervals and using the minimum practical electron doses for image recording (1–2 s exposure at low magnifications and up to 20 s at high magnifications). The liquid layer can also be selectively de-wetted by forming a gas bubble with the electron beam to obtain higher resolution images and then the liquid is re-introduced. The procedure is described in Ref. ²³. This technique enables optimal imaging resolution of the corrosion structures at reduced dose, minimizing beam effects and radiolysis.

The morphologies shown in Figure 1 using LCTEM are similar to corrosion structures observed in previous *ex situ* experiments. Blister formation is known to occur in the early stages of pit formation²⁵. Chloride ions are thought to penetrate the oxide film and cause metal dissolution beneath the oxide-metal interface. This reaction generates hydrogen gas that causes the oxide film to delaminate from the metal and thus forming the blister. As the amount of hydrogen gas increases, the increasing pressure eventually ruptures the blister and exposes the pit to the bulk solution. The formation of fractal-like corrosion patterns in Al thin films has also been studied²⁶. It starts with the perforation of the film by a growing pit. When the pit reaches the inert substrate, propagation has to continue laterally in a two dimensional manner. Morphology of the resulting structures is known depend on the concentration of dissolved ions and can range from round pits to fractal patterns²⁶.

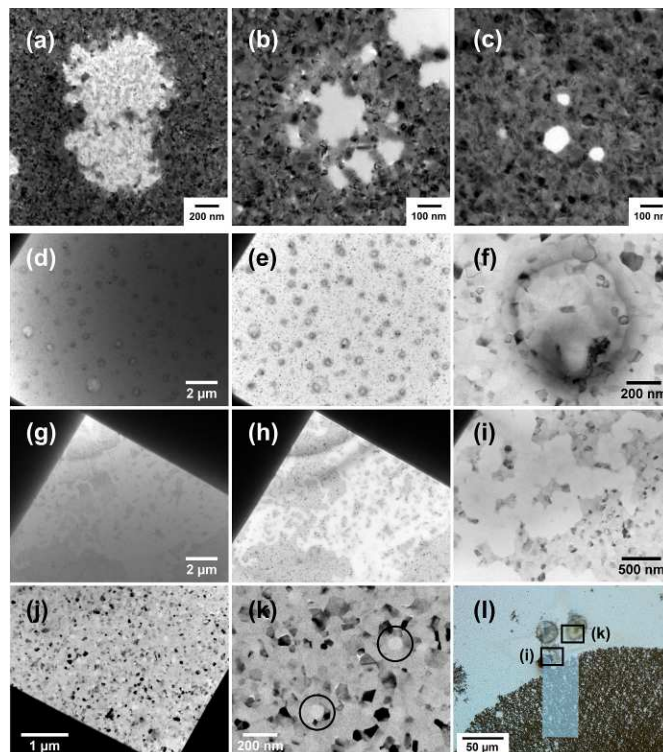


Figure 1. (a-c) Pits at different stages of development observed in 50 nm Cu films after flow of 6 M NaCl solution for 2 hours. (d-f) Blisters formed in a 100 nm Al film after exposure to 0.01 M NaCl solution for 15 hours. (g-i) Meandering corrosion tracks formed in a 100 nm Al film after exposure to 1 M NaCl solution for 4 hours. In (j) and (k), single pits observed in the opposite corner of the windowed area, where in the higher magnification image (k), pits are highlighted with black circles. Images (a-d and g) are obtained with liquid in the cell and (e, f, and h-k) were taken after liquid had been de-wetted with ethanol-water mixtures according to the method given in Ref. ²³. (l) Light microscope image of the window area in the chip with Al film exposed to 1 M NaCl, taken after the experiment. The locations of (i) and (k) are highlighted. It can be seen from (l) that (i) was an extension of a propagating fractal-like corrosion pattern, whereas (k) is taken from a region of intact film. The two circular features are contamination arising from de-wetting of liquid.

The corrosion structures (blisters, fractal patterns, pits) in Figure 1 were obtained by exposing the metallic thin films under open circuit conditions (free corrosion). Pit formation can also be induced by anodic polarization using a potentiostat. Figure 2 shows an *ex situ* bench top example performed in a basic corrosion cell. The cell was fabricated by depositing Al film over the surface of a blank chip, except in the area where it touches the contacts in the holder. This area was selective masked so that only one metal lead touches the film (see diagram in Figure 2(a)). In this case, the reference and working electrodes are made of Ti metal. Depositing a blanket film on blank chips avoids galvanic reactions with the pre-patterned Au electrodes found in electrochemical cells supplied by the manufacturers (discussed further in the ESI†).

The liquid cell was then sealed, a flowing solution of 0.01 M NaCl introduced, and electrochemical experiments carried out on the laboratory bench. The polarization curve in 2(d) shows the expected

behavior for Al in chloride solutions. 2(b, c) compares light microscopy images of the chip before and after the test. Other than a long scratch made during splitting of the cell, it can be seen that corrosion occurred in the form of fractal corrosion networks. These structures are similar to those seen in Figure 1(g-i) at higher solution concentrations without the application of potential. The region of Al under the Ti contact was also often found to be severely corroded. This corrosion at the contact eventually breaks the electrical connection, preventing extended biasing of the samples. Even so, the results demonstrate that this geometry is feasible for electrochemical studies and suggest powerful future opportunities for imaging corrosion under potentiostatic control with improved designs of the corrosion cell.

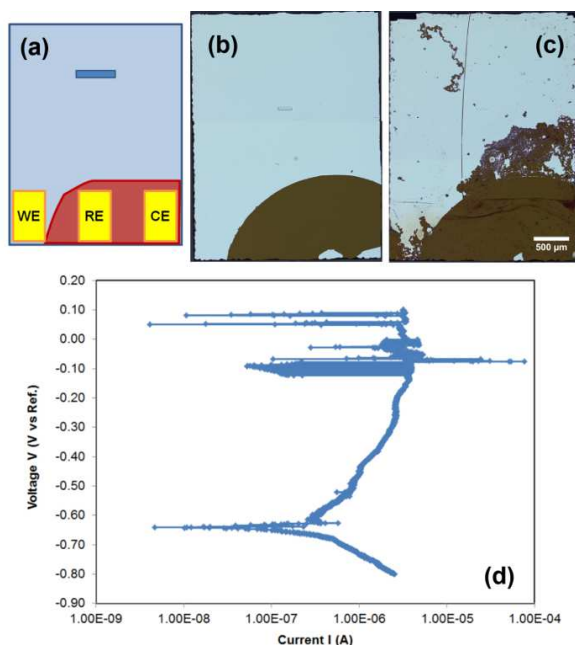


Figure 2. (a) Diagram of the corrosion cell showing the contact regions and electron transparent window (not drawn to scale; WE is the working electrode, RE the reference electrode and CE the counter electrode). (b, c) Light microscope images of the Al coated chip before and after a polarization test. (d) Polarization curve collected from the sample in (b, c). Electrolyte was 0.01 M NaCl, scan range was -0.8 V to 0.1 V, and scan rate was 0.5 mV/s. Fluctuations around 0 V were caused by an overload error in the potentiostat, possibly due to random bubbles adhering to the reference electrode.

Real world corrosion is often initiated at particular sites on a surface where the composition changes or where two dissimilar materials come into contact in an electrolyte. It is therefore of great interest to examine corrosion in thin films patterned with different metals. In liquid cell chips, physical masking is challenging to implement because of the small area accessible to the electron beam. However, focused ion beams can be used to pattern features with dimensions in the tens of nanometers to micrometers, such that several features can be observed in the electron transparent window. In Figure 3 we show a 100 nm thick Al film that has been implanted with Au^+ ions in an array of spots (5 μm spot to spot separation) using a mass-separated focused ion beam column. Under the conditions used, Au^+ ions have a range of about 19 nm (according to SRIM²⁷ simulations) and the implanted ions add less than 1% Au to the entire 450 x 450 μm implanted area. After immersing the sample in 0.1 M NaCl solution

for 3 hours, it is clear that corrosion is modulated by the patterning. In Figure 3(a) and (b), the implanted pattern is reproduced in the corroded film and darker regions indicate a greater amount of corrosion. In Figure 3(c) and (d), individual pits are resolved, showing that the density of pits within and around the implanted regions is lower than in the surrounding area. Since Au is noble relative to Al, the ion implantation appears to have modified the surface chemistry of the Al film and its susceptibility to pitting. This suggests that useful information can be expected from monitoring the microstructural evolution of corrosion in patterned films *in situ*.

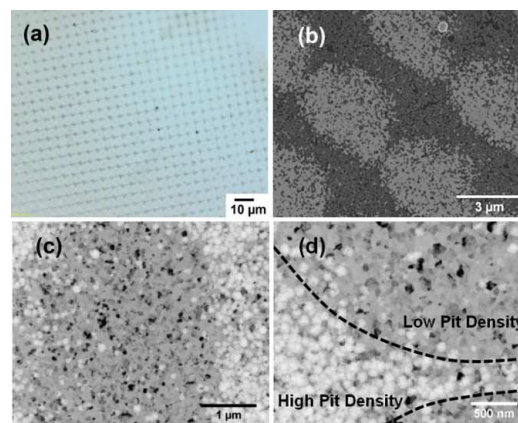


Figure 3. Post-mortem images of an Al film implanted with 30kV Au^+ ions in an array of micrometer-sized spots and then immersed in 0.1 M NaCl solution for 3 hours (not in LCTEM holder). (a) Light microscope image, (b) Scanning electron micrograph at 10kV accelerating voltage and (c, d) TEM bright field images at different magnification, with pits appearing as brighter spots. In (d) the higher and lower pit density regions are demarcated with a dotted line.

Conclusions

We have shown that corrosion experiments carried out *in situ* using liquid cell TEM (LCTEM) can provide information on the onset and development of corrosion morphologies with high spatial and temporal resolution. Corrosion features are visible and can be followed during the evolution of the process. Promising results were achieved using a focused ion beam to modify the surface chemistry and hence pitting sites. Furthermore, polarization curves obtained for Al thin films suggest that LCTEM can provide information on corrosion under an applied bias, given suitable film and electrode geometry. However, it is clear that additional optimization will be beneficial. Further development of these techniques should greatly expand our understanding of fundamental corrosion processes.

S.W.C, D.D., F.M.R. and R.H. acknowledge Dr. Joseph Grogan and Dr. Jeung-Hun Park for discussions on beam effects, Mr. Nicholas Scheidner for modelling the radiolysis species and Ms. Ainsley Pinkowitz for her assistance with electrochemistry experiments. Funding at Rensselaer Polytechnic Institute is provided by the National Science Foundation, grant number DMR-1309509. K.H. and S.H.P acknowledge Ms. Aubrianna Kinghorn and Dr. Bernadette Hernandez-Sanchez for their assistance and the Division of Materials Science and Engineering, the U.S. Department of Energy's Office of Basic Energy Sciences along with Office of Energy and Renewable Energy Water Power Program for partial support. Sandia National Laboratories is a multi-program laboratory managed and operated by Sandia Corporation, a wholly owned subsidiary of Lockheed Martin

Corporation, for the U.S. Department of Energy's National Nuclear Security Administration under contract DE-AC04-94AL85000.

Notes and references

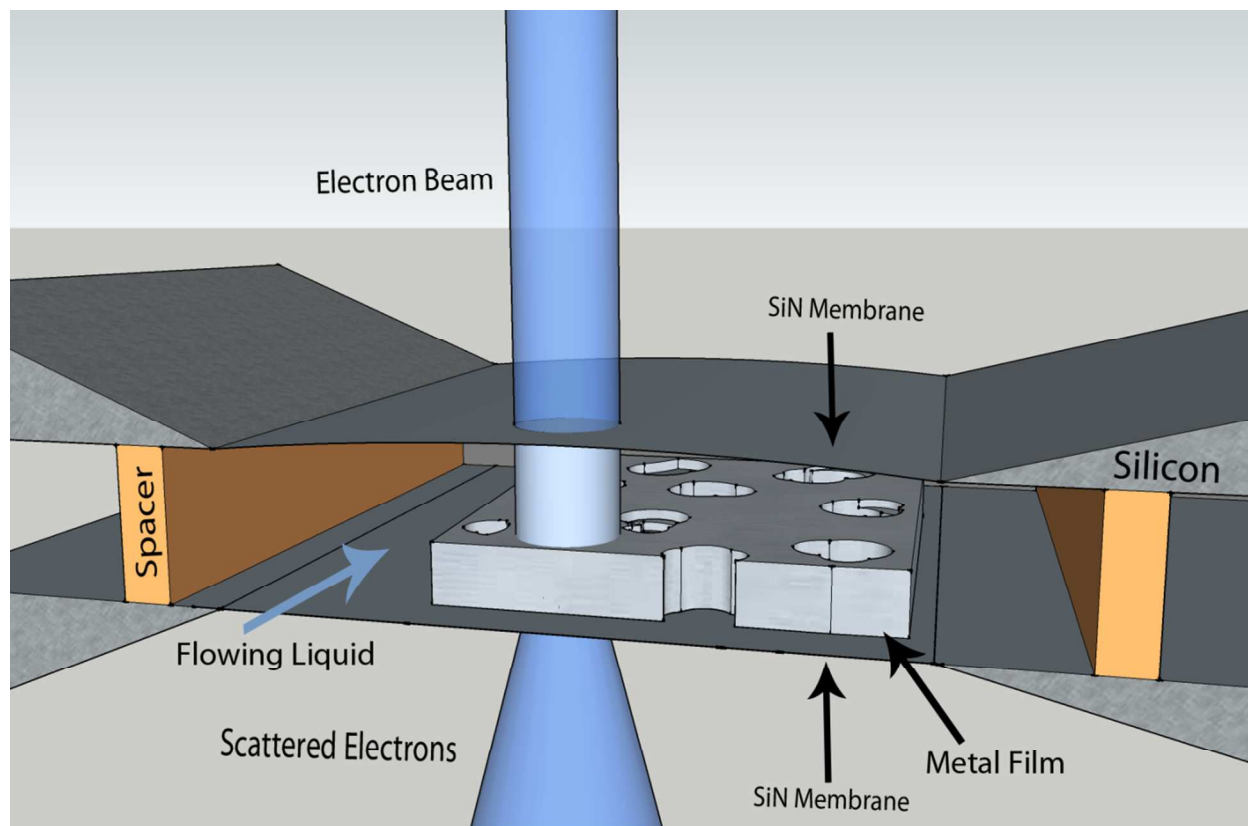
^a Department of Materials Science and Engineering, Rensselaer Polytechnic Institute, Troy, NY 12180.

^b Sandia National Laboratories, Albuquerque, NM 87123.

^c IBM T. J. Watson Research Center, Yorktown Heights, NY 10598.

† Electronic Supplementary Information (ESI) available: Movie S1 showing pit growth in Cu films, details of experimental methods, discussion on design considerations for *in situ* corrosion studies and supplementary figures. See DOI: 10.1039/c000000x/

- M. J. Williamson, R. M. Tromp, P. M. Vereecken, R. Hull, and F. M. Ross, *Nat. Mater.*, 2003, **2**, 532–6.
- M. E. Holtz, Y. Yu, J. Gao, H. D. Abruna, and D. A. Muller, *Microsc. Microanal.*, 2013, **19**, 1027–1035.
- M. Gu, L. R. Parent, B. L. Mehdi, R. R. Unocic, M. T. McDowell, R. L. Sacci, W. Xu, J. G. Connell, P. Xu, P. Abellan, X. Chen, Y. Zhang, D. E. Perea, J. E. Evans, L. J. Lauhon, J.-G. Zhang, J. Liu, N. D. Browning, Y. Cui, I. Arslan, and C.-M. Wang, *Nano Lett.*, 2013, **13**, 6106–6112.
- M. E. Holtz, Y. Yu, D. Gunceler, J. Gao, R. Sundararaman, K. A. Schwarz, T. A. Arias, H. D. Abruña, and D. A. Muller, *Nano Lett.*, 2014, **14**, 1453–9.
- B. Layla Mehdi, M. Gu, L. R. Parent, W. Xu, E. N. Nasybulin, X. Chen, R. R. Unocic, P. Xu, D. A. Welch, P. Abellan, J.-G. Zhang, J. Liu, C.-M. Wang, I. Arslan, J. Evans, and N. D. Browning, *Microsc. Microanal.*, 2014, **20**, 484–92.
- R. L. Sacci, N. J. Dudley, K. L. More, L. R. Parent, I. Arslan, N. D. Browning, and R. R. Unocic, *Chem. Commun.*, 2014, **50**, 2104–7.
- H.-G. Liao, K. Niu, and H. Zheng, *Chem. Commun.*, 2013, **49**, 11720–7.
- G. Frankel, *J. Electrochem. Soc.*, 1998, **145**, 2186.
- G. Frankel and N. Sridhar, *Mater. Today*, 2008, **11**, 38–44.
- K. L. Klein, I. M. Anderson, and N. de Jonge, *J. Microsc.*, 2011, **242**, 117–23.
- N. de Jonge and F. M. Ross, *Nat. Nanotechnol.*, 2011, **6**, 695–704.
- N. J. Zaluzec, M. G. Burke, S. J. Haigh, and M. A. Kulzick, *Microsc. Microanal.*, 2014, **20**, 323–9.
- E. A. Lewis, S. J. Haigh, T. J. A. Slater, Z. He, M. A. Kulzick, M. G. Burke, and N. J. Zaluzec, *Chem. Commun.*, 2014.
- K. L. Jungjohann, J. E. Evans, J. A. Aguiar, I. Arslan, and N. D. Browning, *Microsc. Microanal.*, 2012, **18**, 621–627.
- M. Edwards, J. Ferguson, and S. Reiber, *J. Am. Water Work. Assoc.*, 1994, **86**, 74–90.
- H. Cong, H. T. Michels, and J. R. Scully, *J. Electrochem. Soc.*, 2009, **156**, C16.
- A. El Warraky, H. A. El Shayeb, and E. M. Sherif, *Anti-Corrosion Methods Mater.*, 2004, **51**, 52–61.
- E. Atinault, V. De Waele, U. Schmidhammer, M. Fattahi, and M. Mostafavi, *Chem. Phys. Lett.*, 2008, **460**, 461–465.
- M. Kelm, E. Bohnert, and I. Pashalidis, *Res. Chem. Intermed.*, 2001, **27**, 503–507.
- P. Abellan, T. J. Woehl, L. R. Parent, N. D. Browning, J. E. Evans, and I. Arslan, *Chem. Commun.*, 2014, **50**, 4873–80.
- J. M. Grogan, N. M. Schneider, F. M. Ross, and H. H. Bau, *Nano Lett.*, 2013, **14**, 359–364.
- N. M. Schneider, M. M. Norton, B. J. Mendel, J. M. Grogan, F. M. Ross, and H. H. Bau, *J. Phys. Chem. C*, 2014, **118**, 22373–22382.
- S. W. Chee, F. M. Ross, D. Duquette, and R. Hull, in *MRS Proceedings*, 2013, vol. 1525, pp. mrsf12–1525–ss11–03.
- S. W. Chee, D. J. Duquette, F. M. Ross, and R. Hull, *Microsc. Microanal.*, 2014, **20**, 462–468.
- E. McCafferty, *Corros. Sci.*, 2003, **45**, 1421–1438.
- L. Balazs and J. Gouyet, *Physica A*, 1995, **217**, 319–338.
- J. F. Ziegler, M. D. Ziegler, and J. P. Biersack, *Nucl. Instrum. Meth. B*, 2010, **268**, 1818–1823.



Using liquid cell transmission electron microscopy (LCTEM), localized corrosion of Cu and Al thin films immersed in aqueous NaCl solutions was studied. We demonstrate that potentiostatic control can be used to initiate pitting and that local compositional changes, due to focused ion beam implantation of Au⁺ ions, can modify the corrosion susceptibility of Al films.